CHAPTER VI

ELECTRIC FIELD ASSISTED TRNSDERMAL DRUG DELIVERY FROM SALICYLIC ACID-LOADED POLYACRYLAMIDE HYDROGELS

6.1 Abstract

The apparent diffusion coefficients, D_{app}, and the release mechanisms of salicylic acid from polyacrylamide hydrogels through pigskin were investigated. D_{app} increases with increasing electric field strength and reaches the maximum value at electric field strength of 0.1 V; beyond that it decreases with electric field strength and becomes saturated at 5 V. The increase in D_{app} with low electric field strength can be attributed to the combination of iontophoresis, electroporation of matrix pore, and induced pathway in pigskin. D_{app} obeys the scaling behavior $D_{app}/D_o=(drug\ size/pore\ size)^m$ with m equal to 0.67 and 0.49 for 0 and 0.1 V, respectively.

6.2 Abbreviation

D_{app}	diffusion Coefficient
m_t	amount of drug release at time t
ξ	mesh size
ξe	electrical mesh size
M_c	molecular weight between crosslinks
M_n	the number-average molecular weight of the polymer before crosslinking
$\bar{v}$	the specific volume of PAAM (0.741 mL/g), and
$\bar{V}_1$	the molar volume of water (18.1 mL/mol).
$v_{2,r}$	the polymer volume fraction in the gel in the relaxed state
$v_{2,s}$	the polymer volume fraction in the gel in the swollen state
M_t	the amount of drug released from a hydrogel at time t
M_∞	the total amount of drug released
n	the diffusion scaling exponent, determining the dependence of the

release rate on time that can be related to the drug transport mechanism

a the size of the drug

D_0 the diffusion coefficient as the drug size approaches the mesh size

6.3 Introduction

A number of intelligent drug delivery devices have been proposed to deliver drugs to humans thus providing an effective therapy. Intelligent drug delivery systems (DDS) belong to one expected route in which the systems themselves possess the ability to sense external environmental changes, to judge the degree of external signals, and to release appropriate amounts of drug in response. Among the many possible systems, an intelligent DDS can be fabricated using stimuli-responsive polymeric hydrogels that are capable of altering their structures and physical properties in response to external stimuli such as electric fields, pH, and temperature. Hydrogels have attracted considerable attention as excellent candidates for intelligent DDS due to their swelling behavior, adhesiveness, and biocompatibility (Alvarez *et al.*, 2001; Baljit *et al.*, 2007; and Gil *et al.*, 2002). An electric field is an attractive stimulus because it can be precisely controlled, and the drug delivery responses can be predicted. There is a large body of literature on the use of electric current through the drug matrix, in vivo and in vitro, through the iontophoresis and the electroporation mechanisms (Murdan *et al.*, 2003; Banga *et al.*, 1998). In 1993 Banga *et al.* demonstrated the feasibility of using an electric field to control and predict the release rates of vasopressin from a polyacrylamide (PAAM) hydrogel; they demonstrated that the release of the drug from a hydrogel matrix under electric field strength is faster than the release in the absence of an electric field. Similar behavior was observed for the release of insulin from a polyacrylamide hydrogel (Banga *et al.*, 1993), a protein molecule from a charged polyacrylamide gel (Lewus *et al.*, 1999), and lidocain from poloxamer gels (Chen *et al.*, 1997). In our study, we prepared polyacrylamide hydrogels using N, N′-methylenebisacrylamide (N, N′-MBA) as the crosslinker and ammonium peroxodisulfate as the initiator (Lira *et al.*, 2005). These hydrogels were used as the

drug matrices to study the release dynamics of a model drug, salicylic acid. In particular, we are interested in the effects of electric field and the crosslinking ratio on the drug release rate or the diffusion coefficient of the model drug from these drug-loaded polyacrylamide hydrogels through pigskin and the possible related mechanisms involved.

6.4 Experimental

6.4.1 Materials

Salicylic acid, SA (AR grade, Fluka), was used as the model drug. Acrylamide, AAM (AR grade, Fluka), N,N′ methylenebisacrylamide, (N,N′-MBA) (AR grade, Fluka), tetramethylenediamine, TEMED (AR grade, Fisher Scientific), and ammonium peroxodisulfate (AR grade, Fluka) were used as the monomer, crosslinker, catalyst, and initiator, respectively. Sodium acetate (AR grade, Ajax Chemicals) and glacial acetic acid (AR grade, Carlo Erba) were used without further purification.

6.4.2 Preparation of Salicylic Acid-Loaded Polyacrylamide Hydrogel (SA-loaded PAAM Hydrogel)

The 0.2 %w/w SA-loaded PAAM hydrogels (based on the weight of the acrylamide monomer) were prepared by the free-radical polymerization of 2.32 g of acrylamide in an aqueous solution of salicylic acid (0.0125 M) with N, N′ methylenebisacrylamide (MBA) as crosslinker (Lira *et al.*, 2005). Ammonium persulfate and tetramethylenediamine (TEMED) were used as the initiator and the accelerator. To study the effect of crosslinking ratio on the release of SA from SA-loaded PAAM hydrogels, gels at various crosslink ratios (mol $_{MBA}$: mol $_{AAM}$; 0.002, 0.005, 0.010, 0.016, 0.024) were prepared at various amounts of N, N′ methylenebisacrylamide (MBA). Before gelation (typically after 10 min of mixing the reagents at 27 °C), the pre-gel solution was cast in a mold (diameter 8 cm, thickness 0.5 mm). After gelation, the PAAM hydrogel was cut into a disk shape (diameter ≈ 18 mm, thickness ≈ 0.5 mm).

6.4.3 Characterization of SA-loaded PAAM Hydrogel

To investigate the morphology of the PAAM hydrogel at various crosslink ratios, with and without an electric field, scanning electron micrographs of the hydrogels were taken (JEOL, JSM-5200-2A) using an acceleration voltage of 15 kV and a magnification of 1500. To study the effect of electric field on the PAAM morphology, the hydrogels were swollen in an acetate buffer, at pH 5.5 and attached to a copper electrode. The other electrode was placed elsewhere in the acetate buffer. Samples were prepared from frozen swollen hydrogels with and without electric field in liquid nitrogen and then dried in vacuum at -50°C.

DSC thermograms of the SA, the PAAM hydrogel, and the SA-loaded PAAM hydrogel were recorded (Dupont, DSC 822) to determine their thermal behavior. The 2-4 mg samples were accurately weighed in an aluminum pan with a sealed cover. The measurements were performed under N_2 atmosphere over 30 – 400°C at heating rate of 10°C/min.

The absorption infrared spectra of the PAAM and SA- loaded PAAM hydrogels were measured by an attenuated total reflection Fourier transform infrared spectrometer (ATR-FTIR;Thermo Nicolet, Nexus 670) to investigate the interaction between the salicylic acid and the polyacrylamide hydrogel. The samples were placed on a zinc selenide (ZnSe) crystal sample holder.

To determine the % swelling and the % weight loss of the PAAM hydrogels at various crosslink ratios, they were immersed in an acetate buffer, pH 5.5, at 37 °C. After 24 h the swollen PAAM hydrogels were removed, gently wiped to clean off the surface water, and then re-weighed. To determine the % weight loss, the swollen PAAM hydrogels were dried in a vacuum oven for 5 days until constant weight values were attained. The % swelling and the % weight loss were calculated using the following equations (Proikis *et al.*, 2006):

$$\text{Degree of swelling (\%)} = \frac{M - M_d}{M_d} \times 100 \qquad (6.1)$$

and

$$\text{Weight loss (\%)} = \frac{M_i - M_d}{M_i} \times 100 \qquad (6.2)$$

where M is the weight of a swollen sample, M_d is the weight of swollen sample after drying in vacuum oven, and M_i is the initial weight of the sample (Proikis et al., 2006). All reported data were average values taken from repeated measurements using two specimens.

To determine the mesh size, ξ, the molecular weight between crosslinks, M_c, and the crosslinking density, ρ, of the crosslinked PAAM hydrogels, they were characterized by equilibrium swelling analysis (Lira *et al.*, 2005). Each hydrogel sample (1 cm^2 square) was cut immediately after crosslinking and was weighed in air and heptane (a non-solvent). The particular sample was then placed in deionized water at 37 °C for 5 days for it to swell to the equilibrium size, and was then weighed again in air and heptane. Finally, the sample was dried for 5 days at room temperature and weighed in air and heptane. The average molecular weight between crosslinks of the PAAM gel, M_c, was determined from the swelling data using eq. 6.1 as given by Peppas and Merrill (Peppas *et al.*, 1996):

$$\frac{1}{M_c} = \frac{2}{M_n} - \frac{\frac{\bar{v}}{\bar{V}_1}\left[\ln(1-v_{2,s}) + v_{2,s} + \chi_1 v_{2,s}^{\,2}\right]}{v_{2,r}\left(\left(\frac{v_{2,s}}{v_{2,R}}\right)^{1/3} - \frac{1}{2}\left(\frac{v_{2,s}}{v_{2,r}}\right)\right)} \qquad (6.3)$$

where M_n is the number-average molecular weight of the polymer before crosslinking (determined by using an Ubelodde tube ~ 36,400 g/mol), $\bar{v}$ is the specific volume of PAAM (0.741 mL/g), and $\bar{V}_1$ is the molar volume of water (18.1 mL/mol). $v_{2,r}$ is the polymer volume fraction in the gel in the relaxed state, $v_{2,s}$ is the polymer volume fraction in the gel in the swollen state, and χ is the interaction parameter of PAAM-water, 0.48 (Peppas *et al.*, 1996).

The hydrogel mesh size, ξ, was calculated from the following equation:

$$\xi = v_{2,s}^{-\frac{1}{3}}\left[C_n\left(\frac{2M_c}{M_r}\right)\right]^{1/2} l \qquad (6.4)$$

where C_n is the Flory characteristic ratio for PAAM (8.8), and l is the carbon-carbon bond length (=1.54 Å).

The crosslinking density of the hydrogel was calculated using Eq (6.5) (Peppas *et al.*, 1996):

$$\rho_x = \frac{1}{\nu \overline{M}_c} \qquad (6.5)$$

6.4.4 Release of SA from Crosslinked SA-loaded PAAM Hydrogel Experiments

6.4.4.1 Preparation of Buffer Solution

To prepare 1000 mL of an acetate buffer solution at a pH of 5.5, 15 mL of glacial acetic acid and 150 g of sodium acetate were added to distilled water in a volumetric flask with a total volume of 1000 mL.

6.4.4.2 Pigskin Preparation

In-vitro drug released experiments were performed using Fresh pigskin obtained from the abdominal part. The skin used in this work was about 1-1.5 mm thick. The whole pigskins were surgically removed and cleaned with normal sterile saline. The subcutaneous fat, tissue, blood vessels, and epidermal hair were carefully removed by blunt section. The skin was free of obvious holes or defects. The complete skin was cleaned with saline and finally with distilled water, cut into a circle, wrapped with aluminium foil, and stored in a frozen state. In the drug release experiment, pigskin was soften at room temperature before use.

6.4.4.3 Spectrophotometric analysis of the model drug

A UV/visible spectrophotometer (Shimadzu, UV-2550) was Used to determine the maximum spectra of model drug. Model drug in aqueous solution was prepared for determining the maximum absorption wavelength. The characteristic peak was observed. The absorbance value at the maximum wavelength of 296 nm of the model drug was read and the corresponding model drug concentrations were calculated from the calibration curve.

6.4.4.4 Actual Amount of Drug Content

The actual amount of SA in the SA-loaded PAAM hydrogel (circular disc about 1.8 cm in diameter) was determined by dissolving the sample in 4 ml of dimethyl sulfoxide (DMSO), and 0.5 ml of the solution was added to 8 ml of the acetate buffer solution. The drug amount in the dilute solution sample was measured by using a UV/Visible spectrophotometer at a wavelength of 296 nm and through a predetermined calibration curve. It should be noted that the presence of DMSO in the dilute solution has no apparent effect on the UV absorbance at the wavelength of 296 nm. The data are reported here as an average taken from at least three measurements.

6.4.4.5 Transdermal transport studies

Transdermal diffusion through a hairless pigskin was carried out in order to study the release characteristics of the drug from a SA-loaded PAAM hydrogel. A hairless pigskin (thickness ~ 1-1.5 mm) was placed on top of the acetate buffer solution on a custom built modified Franz diffusion cell. The area available for permeation was 3.14 cm^2. The pigskin was allowed to come into equilibrium contact with the acetate buffer (pH 5.5, ionic strength of 0.001225 M) in the receptor chamber; the buffer was magnetically stirred throughout the experiment period (48 h) at a thermostatically maintained temperature (37 ± 2 °C). The SA-loaded PAAM hydrogel with a particular crosslinking ratio (0.002, 0.005, 0.016 or 0.024) was placed between the copper cathode and the pigskin, which was mounted onto the receptor compartment. To study the effect of electric field strength on the release of the SA from the SA-loaded PAAM hydrogel, the cathode electrode (copper electrode) was connected to a power supply (KETHLEY 1100V Source Meter), which provided various electrical voltgaes (V = 0, 0.01, 0.03, 0.05, 0.07, 0.1, 0.5, 1.0 and 5.0 V) across the SA-loaded PAAM hydrogel, the pigskin, and the buffer solution. The anode electrode pin was positioned in the buffer solution. The duration of applying the electric field to the experiemtntal setup is ~48 h. The donor and receiver compartments were kept in contact by wrapping parafilm at the junction. The total diffusion period investigated was 48 h, 0.3 ml of the buffer solution was withdrawn and an equal amount of fresh buffer solution was added to the cell, every

15 minutes during the first hour, to ensure good contact between the buffer solution and the skin at all times. The amount of the drug in the withdrawn solution samples was determined using a UV spectrophotometer at 296 nm. The data were then analyzed to determine the cumulative amount of the drug released from the samples at each specified diffusion period. The experiments were carried out in triplicate and the data were reported as average values.

6.5 Results and Discussion

6.5.1 Characterizations

PAAM was chemically polymerized through the free radicalization and subsequently crosslinked at 27 °C (Fernandez *et al.*, 2005). The molecular weight between crosslinks, the mesh size, and the crosslinking density are parameters (Eqs. 6.3-6.5) used for characterizing the porous structure of the hydrogel for the drug delivery system. These parameters are determined from equilibrium swelling studies in distilled water were carried out to characterize the gels at 37 °C as described previously by Peppas and Barr-Howell (Peppas *et al.*, 1996). Table 6.1 gives the molecular weights between crosslinks, M_c, the mesh size, ξ, and the crosslinking density for each hydrogel in terms of crosslinking ratio, with and without electric field. It can be seen that as the crosslinking ratio decreases, the mesh size and the molecular weight between crosslink increases. As the amount of crosslinking agent decreases, the spacing between the crosslinks becomes wider and the strand becomes longer. The mesh sizes of hydrogels are between 57 – 252 Å at electric field strength of 0 V, and between 119 – 348 Å at electric field strength of 0.1 V. Thus, the increase in the mesh size of the system with electric field on suggests that the electric field has apparent effect on the PAAM structure. The phenomenon of electro-induced gel swelling rarely occurs relative to that of gel deswelling and more work needs to be done before it is fully understood (Murdan *et al.*, 2003). In our work, the electro-induced gel swelling at low voltage (less than 0.1 V) might be explained by the electrically-induced ionization of the amide groups in PAAM hydrogel. When an electric field is applied to an aqueous medium, the positive ions (H^+) in aqueous medium migrate toward cathode side. H^+ ions penetrate into PAAM hydrogel on

their way to the cathode side. This induces the ionization of the amide groups on PAAM hydrogel and causes the gel on the cathode side to swell as the ionized groups become hydrated (Murdan *et al.*, 2003).

Scanning electron micrographs of PAAM hydrogels at various crosslinking ratios are shown in Figure 6.1. The mesh sizes observed from the micrographs can be correlated with the data calculated from the M_c; as the crosslinking ratio decreases, the mesh size increases. The mesh sizes, as determined visually from the micrographs are: PAAM_0.002 (8.29 ± 3.95 μm); PAAM_0.005 (7.04 ± 2.76 μm); PAAM_0.010 (6.53 ± 1.92 μm); PAAM_0.016 (4.18 ± 1.30 μm); and PAAM_0.024 (2.85 ± 1.30 μm). These values are higher than the intrinsic mesh sizes calculated from equation 2 by two orders of magnitude. We should note that mesh sizes as determined from the SEM micrographs are "apparent" mesh sizes, appearing at the surfaces, whereas the mesh sizes from M_c are effective bulk pore sizes.

In this present work, the degree of swelling is related to the amount of gel required to achieve a suitable. As expected intuitively, the degree of swelling is inversely proportional to the degree of crosslinking. The % of swelling of PAAM hydrogels at these various crosslinking ratios at 37°C are 747 ± 12 for PAAM_0.002, 526 ±24 for PAAM_0.005 , 453 ± 3 for PAAM_0.010, 391 ± 20 PAAM_0.016, and 347 ±7 for PAAM_0.024. The % of weight loss are 16.5 ± 1.5 for PAAM_0.002, 15.8 ± 1.9 for PAAM_0.005, 14.6 ± 1.4 for PAAM_0.010, 10.9 ± 1.9 for PAAM_0.016, and 7.25 ±0.95 for PAAM_0.024. The data show that the % of swelling and the % of weight loss monotonically decrease with increasing crosslinking ratio. These results are consistent with theoretical predictions which describe the swelling of gel as a function of the degree of crosslinking (Wang *et al.*, 1993).

IR spectra of SA-loaded PAAM hydrogels are shown in comparison with that of pure PAAM hydrogel in Figure 6.2 in order to identify the interactions between SA and the PAAM hydrogel matrix. For the pure PAAM hydrogel, peaks at 3340, 3328, and 1434 cm^{-1} can be observed. These characteristic peaks of pure PAAM can be assigned to the vibrations of N-H, NH_2, and CN, respectively. Peak at 1670 cm^{-1} corresponds to the vibration of C=O group of acrylamide/MBA

Windows XP Printer Test Page

Congratulations!

If you can read this information, you have correctly installed your HP LaserJet 1020 on CHENGGIECHENG.

The information below describes your printer driver and port settings.

Submitted Time: 12:15:58 20/10/2551
Computer name: CHENGGIECHENG
Printer name: HP LaserJet 1020
Printer model: HP LaserJet 1020
Color support: No
Port name(s): USB001
Data format: RAW
Share name:
Location:
Comment:
Driver name: IMFNT5.DLL
Data file: SDhp1020.DLL
Config file: SDNT5UI.DLL
Help file: SDhp1020.HLP
Driver version: 5.06
Environment: Windows NT x86
Monitor: HPLJ1020LM
Default datatype: RAW

Additional files used by this driver:

C:\WINDOWS\System32\spool\DRIVERS\W32X86\3\SDhp1020.DLL (5, 6, 1516, 0)
C:\WINDOWS\System32\spool\DRIVERS\W32X86\3\SUhp1020.dll (5, 60, 2208, 0)
C:\WINDOWS\System32\spool\DRIVERS\W32X86\3\SUhp1020.ent
C:\WINDOWS\System32\spool\DRIVERS\W32X86\3\ZJBIG.dll (5, 4, 334, 3)
C:\WINDOWS\System32\spool\DRIVERS\W32X86\3\ZLhp1020.dll (5, 53, 3723, 0)
C:\WINDOWS\System32\spool\DRIVERS\W32X86\3\SUxml.dll (5, 60, 2513, 0)
C:\WINDOWS\System32\spool\DRIVERS\W32X86\3\xerces-c.dll (1, 7, 0)
C:\WINDOWS\System32\spool\DRIVERS\W32X86\3\hp1020.img
C:\WINDOWS\System32\spool\DRIVERS\W32X86\3\hp1022.img
C:\WINDOWS\System32\spool\DRIVERS\W32X86\3\hp1022n.img
C:\WINDOWS\System32\spool\DRIVERS\W32X86\3\zshp1020.exe (1, 0, 1118, 0)
C:\WINDOWS\System32\spool\DRIVERS\W32X86\3\ZSHP1020.HLP
C:\WINDOWS\System32\spool\DRIVERS\W32X86\3\SUHP1020.VER
C:\WINDOWS\System32\spool\DRIVERS\W32X86\3\vshp1020.dll (1, 0, 1026, 0)
C:\WINDOWS\System32\spool\DRIVERS\W32X86\3\IMFPRINT.DLL (5, 54, 336, 0)
C:\WINDOWS\System32\spool\DRIVERS\W32X86\3\QDPRINT.DLL (5, 52, 1018, 0)
C:\WINDOWS\System32\spool\DRIVERS\W32X86\3\Sd32.dll (5, 60, 2216, 0)
C:\WINDOWS\System32\spool\DRIVERS\W32X86\3\SDIMF32.DLL (5, 60, 2209, 0)
C:\WINDOWS\System32\spool\DRIVERS\W32X86\3\SDIMGR.DLL (6, 60, 2228, 0)
C:\WINDOWS\System32\spool\DRIVERS\W32X86\3\SDDMUI.DLL (6, 1, 524, 0)
C:\WINDOWS\System32\spool\DRIVERS\W32X86\3\SDUI.DLL (6, 0, 1520, 1)
C:\WINDOWS\System32\spool\DRIVERS\W32X86\3\ZGDI32.DLL (5, 60, 709, 0)
C:\WINDOWS\System32\spool\DRIVERS\W32X86\3\SUhp1020.ini
C:\WINDOWS\System32\spool\DRIVERS\W32X86\3\ZSPOOL.DLL (5, 51, 709, 0)
C:\WINDOWS\System32\spool\DRIVERS\W32X86\3\ZSPOOL95.EXE (5, 60, 1112, 0)
C:\WINDOWS\System32\spool\DRIVERS\W32X86\3\ZTAG32.DLL (5, 60, 1210, 0)
C:\WINDOWS\System32\spool\DRIVERS\W32X86\3\ZUNINST.EXE (2, 0, 2027, 0)
C:\WINDOWS\System32\spool\DRIVERS\W32X86\3\zlm.dll (5, 50, 1416, 0)
C:\WINDOWS\System32\spool\DRIVERS\W32X86\3\IMF32.DLL (5, 60, 2204, 0)
C:\WINDOWS\System32\spool\DRIVERS\W32X86\3\SDNTUM4.DLL (5, 0, 508, 0)

This is the end of the printer test page.

(crosslinker) unit which provide an evidence for the successful crosslinking of polyacrylamide. There are two bands associated with the N-H stretching vibration, one is located at ~3,190 cm^{-1} (hydrogen bonded N-H stretching), and another band is located at 3340 cm^{-1} (non-hydrogen bonded N-H stretching) (Tao *et al.*, 2005). For pure PAAM, the 3190 cm^{-1} band is negligible in comparison with the intense 3440 cm^{-1} band. For the 0.2% salicylic acid-loaded PAAM hydrogels, changes in the IR spectrum can be observed. The band at 3190 cm^{-1} can be assigned to the hydrogen bonding between the N-H of PAAM and the OH of salicylic acid. For the 1.5% salicylic acid-loaded PAAM hydrogel, the spectrum shows that the hydrogen bonding between the N-H of PAAM and the OH of salicylic acid (3190 cm^{-1}) becomes quite evident. This suggests the H-bonding between the N-H of PAAM and the OH of salicylic acid (Tao *et al.*, 2005).

DSC thermograms of SA, SA-loaded PAAM hydrogel, and PAAM hydrogel were measured to investigate the interaction between salicylic acid and the polyacrylamide matrix. The melting temperature (T_m) of PAAM is 231 °C, consistent with previous study (Sahiar *et al.*, 2006). However, the T_m of PAAM in SA-loaded PAAM occurs at 225 °C, suggesting that SA possibly interacts with the PAAM hydrogel through hydrogen bonding between the hydroxyl groups of the SA and the amine groups of the PAAM hydrogel. In summary, the thermal properties of the salicylic acid-loaded PAAM support the FTIR results on the interaction.

6.2.2 Release Parameters and Kinetics of SA from SA-loaded PAAM Hydrogel

We first investigate the actual amount of drug within the sample, which is reported as the percentage of the initial content of drug loaded into the PAAM solution (0.938 g of SA). The actual amounts of drug present in the samples after gelation are about 92.1 ± 7.1%.

In order to study the SA transport mechanism from the PAAM hydrogels through diffusion, various diffusion models are used to analyze the experimental data. The amount of drug released from a hydrogel at time t (M_t) with

respect to the total amount of drug released (M_∞), can be expressed in terms of a power law of time as follows:

$$\frac{M_t}{M_\infty} = kt^n, \tag{6.6}$$

where n is the diffusion scaling exponent. The value of n determines the dependence of the release rate on time that can be related to the drug transport mechanism. The drug transport mechanisms can be identified as Fickian, non-Fickian (anomalous), linear (zero order), and super case II transport when n is equal to 0.5, $0.5<n<1.0$, 1.0 and $n>1.0$, respectively (Korsmeyer *et al.*, 1983).

In particular, the Higuchi's equation (Korsmeyer *et al.*, 1983) is associated with the Fickian diffusion of the drug:

$$\frac{M_t}{M_\infty} = k_H t^{0.5}, \tag{6.7}$$

where M_t/M_∞ is the fractional drug released, k_H is a kinetic constant, and t is the release time.

The apparent diffusion coefficients, D_{app}, of SA from the SA-loaded PAAM hydrogels through the pigskin incorporates the physical characteristics of the matrix/drug system as well as some physical contributions from the measurement methods (namely in the case of the transdermal diffusion through a pigskin method, which involves the additional permeation of the drug through a pigskin) are determined and investigated here. Each D_{app} value is calculated from the slope of the amount of released drug vs. the square root of time during the initial period, according to the Higuchi's equation (Ferreira *et al.*, 2001):

$$Q = 2C_0(D_{app}t/\pi)^{1/2}, \tag{6.8}$$

where Q is the amount of drug released per unit area, C_0 is the initial drug concentration in the gel, and D_{app} is the apparent diffusion coefficients diffusion coefficient of a diffusant (Ferreira et al., 2001). We may note D_{app} obtained from Eqs. (6.7) and (6.8) are valid over an initial period of time and based on the Fick's laws.

6.5.2.1 Effect of Crosslinking Ratio

In our work, the release characteristic of SA from SA-loaded PAAM, which refers to the transdermal diffusion from the hydrogel matrix and the subsequent permeation through the pigskin, was investigated. The experiments were carried out using an acetate buffer as the transferring medium at the physiological temperature of 37 °C. The amounts of SA released from SA-loaded PAAM hydrogels of various crosslinking ratios (PAAM_0.002, PAAM_0.005, PAAM_0.010, PAAM_0.016, PAAM_0.024) in the absence of an electric field during a 48 h period are shown as functions of t and $t^{1/2}$ in Figures 6.3 and 6.4 respectively. The amount of SA released ($C_6H_4(OH)CO_2H \Leftrightarrow C_6H_4(O^-)CO_2H + H^+$) from the SA-loaded PAAM hydrogels through the pigskin increases very rapidly over the first 6 hours; after that period it increases gradually until reaching equilibrium. The amount of salicylic released through pigskin was reported as the percentage of the actual amounts of drug in the PAAM sample (~ 0.89 mg of SA). The percentages of SA released from the SA-loaded PAAM are 72, 70, 56 and 44% for PAAM_0.002, PAAM_0.005, PAAM_0.010 and PAAM_0.016, respectively. Evidently, the amount of SA released from SA-loaded PAAM through the pigskin is greater at a given time for samples with a lower crosslinking ratio. We also investigate the amount of drug residue within the sample, which is reported as the percentage of the actual amounts of drug in the PAAM sample (~ 0.89 mg of SA). The amounts of drug residue in the samples after released are 14, 16, 32, and 43% for PAAM_0.002, PAAM_0.005, PAAM_0.010, and PAAM_0.016, respectively.

From our data of Figure 6.3 and a plot of $\ln(M_t/M_\infty)$ vs. $\ln(t)$ over total experimental period 48 h, the scaling exponent n of Eq. (6) was determined. The n value of PAAM_0.002 is 0.43 close the Fickian exponent value of n = 0.5. Thus the amounts of SA released are predominantly controlled by the Fickian diffusion mechanism. For crosslinked PAAM without applying electric field, the scaling exponent n increases from 0.43, 0.50, 0.50, 0.54 to 0.93 for PAAM hydrogels with crosslinking ratios of 0.002, 0.005, 0.010, 0.016 and 0.024, respectively. Therefore, the drug release, without applying electric field, deviated

further from the Fickian diffusion towards the anomalous case as crosslinking ratio is increased.

The kinetic constant k decreases from 0.232, 0.140, 0.099, 0.072 to 0.015 (hr^{-n}) for PAAM hydrogels with crosslinking ratios of 0.002, 0.005, 0.010, 0.016 and 0.024, respectively. The release rate is slower with the samples with a higher crosslinking ratio, apparently due to the smaller pore size (Sairam *et al.*, 2006) as shown in the SEM micrographs of Figure 6.1. In addition, the smaller % swelling may further hinder the amount of salicylic acid released from the hydrogel.

Figure 6.5 shows the D_{app} of SA from SA-loaded PAAM hydrogel through pigskin versus the crosslinking ratio and the mesh size at electric field strengths of 0 and 0.1 V, at 37 °C. The data suggest that D_{app} evidently decreases with increasing crosslink ratio due to the reduction in the matrix pore size (Ferreira *et al.*, 2001). As an electric field is applied, D_{app} increases by a factor of two at a given crosslink ratio or pore size. At an electric field strength of 0.1 V, the dependence of D_{app} on the crosslink ratio or the pore size is similar to that without the electric field turned on. The increase of D_{app} under electric field will be discussed further under the effect of electric field strength part.

Table 6.2 shows the diffusion coefficients of drugs from PAAM hydrogels at various conditions. The diffusion coefficients of drug from PAAM hydrogels are larger at lower crosslinking ratios (smaller mesh size) or larger drug size.

Ferreira *et al.* (2001) studied the effect of crosslinking ratio on the diffusion coefficients of acetylsalicylic acid (drug size ~ 3.01 Å) from polyacrylamide hydrogels without an electric field. The acetylsalicylic acid loaded polyacrylamide was immersed in fresh deisstilled water with megnatic stirring for 15 min at 37 °C to study the release characteristic of acetylsalicylic acid from acetylsalicylic acid loaded polyacrylamide. The diffusion coefficient generally decreases with increasing crosslink ratio due to decreasing matrix pore size. The diffusion coefficients of acetylsalicylic acid are 1.2×10^{-7} and 8.5×10^{-8} cm^2s^{-1} for the crosslinking ratios (mol_{MBA}/mol_{AAM}) of 0.0115 and 0.02305, respectively (Ferreira *et al.*, 2001).

Valento *et al.* (2002) reported a similar effect of crosslinking ratio on the diffusion coefficients of sodium dodecyl sulfate, SDS (drug size ~ 20 Å) in water-swollen crosslinked polyacrylamide membranes in the absence of an electric field. The diffusion of SDS through polyacrylamide hydrogel was measured by using the cell that consists of two components filled with SDS solution and water, respectively. The polyacrylamide hydrogel was placed between 2 cells. The diffusion coefficient apparently decreases with increasing crosslink ratio due to a decreasing matrix pore size. The diffusion coefficients of sodium dodecyl sulfate are 0.5 x 10^{-6}, 1.2 x 10^{-6}, and 2.5 x 10^{-6} cm^2s^{-1} for crosslinking ratios (mol_{MBA}/mol_{AAM}) of 0.032, 0.0032, and 0.0014, respectively (Valento *et al.*, 2000).

From these previous reports, it appears that the diffusion coefficients of acetylsalicylic acid and sodium dodecyl sulfate through PAAM membranes are higher than the apparent diffusion coefficients of SA from our SA-loaded PAAM hydrogels through the pigskin. The diffusion of acetylsalicylic acid and sodium dodecyl sulfate are driven by osmotic pressure. In our case, the diffusion of SA is driven by the concentration gradient in the absence of an electric field. Thus the diffusion coefficient of release drug strongly depends on drug size, mesh size of hydrogel.

Figure 6.6 shows the log-log plot of the D_{app} of SA from SA-loaded PAAM hydrogel vs. drug size/mesh size ratio of hydrogels at electric field strengths of 0 and 0.1 V, at 37 °C. From the mesh size of the hydrogel in an absence of electric field and under electric field (ξ and ξ_e) data, the diffusion coefficient follows the scaling behavior as follows:

$$D_{app} = D_0 (a/\xi)^{-m}, \tag{6.9}$$

where D_{app} is the apparent diffusion coefficient of the drug, D_0 is the diffusion coefficient as the drug size approaches the mesh size, a is the size of the drug, ξ is the mesh size of the hydrogel, and m is the scaling exponent. By using the mesh size of the hydrogel in an absence of electric field data, the scaling exponent m value for the SA diffusion through the polyacrylamide matrix and the pigskin under electric field strengths of 0 and 0.1 V are 0.67 and 0.36, respectively. Corresponding D_o values are 1.16 x 10^{-9} and 8.89 x 10^{-9} cm^2/s, respectively. When an electric field is

applied to a polyacrylamide hydrogel, the mesh size of polyacrylamide hydrogel is expanded to ξ_e. The scaling exponent m value for the SA diffusion through the polyacrylamide base on ξ_e under electric field strength of 0.1 V is 0.49. Coresponding D_0 is 3.84 x 10^{-9} cm^2/s. The scaling exponent *m* value for the SA diffusion through the polyacrylamide matrix and the pigskin under electric field strengths of 0.1 V based on ξ_e is believed to be more accurate in reflecting the actual diffusion under electric field. From our data, the SA released from SA-loaded PAAM hydrogel is controlled by the Fickian diffusion mechanism. The changes in the PAAM structure and the matrix pore size and in the SA/PAAM interaction through an electric field evidently are responsible for the difference in the diffusion scaling exponent *m* under an electric field.

6.5.2.2 Effect of Electric Field Strength

We next investigate the effect of electric field strength on the release characteristics of SA from SA-loaded PAAM hydrogels through the pigskin with a fixed crosslinking ratio of 0.016: PAAM_0.016. Figure 6.7 shows the amounts of SA released versus the square root of time of the PAAM_0.016 at various electric field strengths, 0 – 0.1 V (low voltage); the sample was attached to the negatively charged electrode (cathode). From Figure 6.7, the amount of SA released is clearly greater as electric field strength is applied as a higher electrical current, or higher electrostatic force, is present driving the negatively charged drug through the polymer matrix (Murdan *et al.*, 2003 and Kantaria *et al.*, 1999). It is known that the amount of drug delivery across the skin is proportional to the applied current and the duration of applying electric field (Sage *et al.*, 1992). The second driving force possibly comes from the expansion of the matrix PAAM hydrogel pore size from 4.18 ± 1.30 μm (E= 0 V) to 9.3 ± 4.8 μm (E = 0.1 V), as visualized in Figure 6.1 (c) and (d), respectively. In addition, the electric field can increase the permeation of the hydrophilic drug, SA, through the liophilic stratum corneum in the pigskin by the creation of transient micropores in the skin which provide the transport pathway of the drug (Gusbeth *et al.*, 2000; Huang *et al.*, 2005 and Murdan *et al.*, 2003). .

Data of Figure 6.7 were fitted to Eq. (6.6) and the scaling exponent n of crosslinked PAAM (PAAM_0.016) was determined to be n ≈ 0.34 – 0.54. For

crosslinked PAAM (PAAM_0.016) at various electric field strengths, the scaling exponent n decreases from 0.54, 0.53, 0.43, 0.37 to 0.34 at electric field strengths of 0, 0.01, 0.05, 0.07, and 0.1 V, respectively. Thus, under applied electric field, the diffusion deviates from the anomalous case towards the Fickian diffusion as electric field strength increases.

The kinetic constant k increases from 0.071, 0.090, 0.131, 0.207 to 0.250 (hr^{-n}) for PAAM_0.016 at electric field strength sof 0, 0.01, 0.05, 0.07, and 0.1 V, respectively. The release rate is accelerated under appliedelectric field because of the electrophoresis effect driving SA, the expansion of pore size, and the creation of transient pathways in the pigskin as discussed before.

Figure 6.8 shows the D_{app} of SA from SA-loaded PAAM hydrogels at a crosslink ratio of 0.016, PAAM_0.016, through the pigskin versus electric field strength, at 37 °C as determined from data of Figure 6.7 using eq. 6.8. D_{app} initially increases with increasing electric field strength and reaches a maximum value at an electric field strength of 0.1 V; beyond that it decreases with electric field strength and becomes saturated at an electric field strength of 5 V. In summary, we can state that D_{app} increases at low electric field strength (less than 0.1 V) due to the expansion of the matrix pore size, the electrophoresis of the anionic drug, and the creation of pathways in the pigskin. For an electric field strength higher than 0.1 V, the decrease in the D_{app} is due to the decrease in the polyacrylamide pore size from 9.3 ± 4.8 μm (E = 0.1 V) to 4.50 ± 1.75 μm (E = 5 V), as shown in Figure 4 (d) and (e), respectively. The contraction of pore size results from a sufficiently high electric field strength being capable of creating electrolysis in the buffer solution. When an electric field is applied to an aqueous medium, the electrolysis in buffer solution produces positive and negative buffer ions. The negative buffer ions are generated at cathode electrode, resulting in the deprotonation and the neutralization of positive charged groups on the PAAM and consequently gel de-swelling at cathode (Gusbeth *et al.*, 2000 and Huang *et al.*, 2005). Tanaka *et al.*, also reported that the de-swelling of partially hydrolyzed PAAM hydrogel occurred continuously along the gel axis when an electric field of 1.25 V was applied, and the de-swelling increased with voltage. As the gel de-swells, the reticular size of the polymer network is reduced.

The drug pathway out of the gel becomes more tortuous, leading to the decrease in the diffusion coefficient (Murdan *et al.*, 2003 and Tanaka *et al.*, 1982). As the electric field strength is higher than 5.0 V, D_{app} becomes saturated with electric field; it is possible that at higher voltages the gel contraction balances out the electrophoresis effect, or the gel resistance to the crossing of charge increases as the content of free water increases (Murdan *et al.*, 2003).

Chen L. *et al.* (1996) determined the diffusion coefficient of luteinizing hormone, LHRH from PAAM hydrogel and abdominal hairless rat skin when an electric field was applied by using the iontophoretic permeation cell. The abdominal skin was mounted onto one opening of the iontophoretic permeation cell; LHRH-loaded polyacrylamide was mounted onto the abdominal skin and dorsal skin was mounted onto other opening. A LHRH-free reservoir device was attached to the dorsal skin to complete the experimental setup. An anionic electrode was applied to a LHRH-loaded polyacrylamide reservoir device. A cathodic electrode was applied to the LHRH-free reservoir device to complete the circuit. As an electric field strength of 3.0 V (0.6 mA) was applied, the diffusion coefficient of the luteinizing hormone was 1.64×10^{-7} cm^2s^{-1} for a crosslinking ratio (mol_{MBA}/mol_{AAM}) of 0.0115 (Chen *et al.*, 1996). The diffusion coefficients of the luteinizing hormone through the PAAM hydrogel and the abdominal hairless rat skin in their work are higher than the diffusion coefficients of salicylic acid through our PAAM hydrogels and the pigskin. This may originate from the lower potential to form interaction between PAAM hydrogel and the luteinizing hormone, and the higher diffusability of the drug through the abdominal hairless rat skin; thus a larger diffusion coefficient was obtained. In general, we may conclude that the diffusion coefficient of a drug in transdermal delivery system depends on several factors: the chemical composition of the drug, the molecular weight of the drug, and the size of the drug, the polymer matrix, the drug-matrix interaction, and the experimental set up, as shown in Table 2 (Ferreira *et al.*, 2001; Valento *et al.*, 2000; Chen *et al.*, 1996; Attwood *et al.*, 1981 and Vankov *et al.*, 2004), and a further studied is needed.

6.6 Conclusion

The SA-loaded polyacrylamide hydrogels were prepared by varying the crosslinking ratio to study the release mechanism and the apparent diffusion coefficient, D_{app}, of the model drug from drug-loaded PAAM hydrogels with and without an electric field. Regarding the effect of crosslinking ratio, the D_{app} decreases with increasing crosslink ratio due to the larger pore size with the lower crosslink ratio. Regarding the effect of electric field strength, the D_{app} increases with increasing electric field strength and reaches the maximum value at an electric field strength of 0.1 V; it then decreases with further electric field strength increase and becomes saturated at an electric field strength of 5.0 V. The increase in D_{app} at low electric field strength is due to the electrophoresis effect driving the SA, the expansion of pore size, and the creation of transient pathways in the pigskin. D_{app} decreases at high voltage, due mainly to the contraction of pore size resulting from the electrolysis of buffer solution. The negative buffer ions are generated at the cathode electrode, resulting in the deprotonation and the neutralization of positive charged groups of PAAM. It is possible to conclude that by varying crosslinking density, the electric field strength, the drug size and the hydrogel matrix pore size, and the drug-matrix interaction the drug release rate can be precisely controlled towards an optimal desired level.

6.7 References

Alvarez-Figueroa, M.J. and Blanco-Méndez, J. (2001). Transdermal delivery of methotrexate: iontophoretic delivery from hydrogels and passive delivery from microemulsions. Int J Pharm 215:57-65.

Attwood, D., Johansen, L., Tolley, J. and Rassing, J. (1981). A new ultrasonic method for the measurement of the diffusion coefficient of drugs within hydrogel matrics, Int J Pharm 9:285 -94.

Baljit, S., Chauhan, G.S., Sharma, D.K. and Chauhan, N. (2007). The release dynamics of salicylic acid and tetracycline hydrochloride from the psyllium and polyacrylamide based hydrogels (II). Carbohyd Polym 67(4): 559-65.

Banga, A.K. (1998). Electrically Assisted Transdermal and Topical Drug Delivery, Taylor&Francis ltd., Canada .

Banga, A.K., Chien, Y. (1993). Hydrogel-based iontotherapeutic delivery devices for transdermal delivery of peptide/protein drug, Pharm Res 10(5):679-702.

Chen, L. and Chien, Y. (1996). Transdermal iontophoretic permeation of luteinizing hormaine releasing hormone: characterization of electric parameters. J Control Release 40:187-98.

Chen, W., Frank, S.G. (1997). Iontophoresis of lidocane H^+ From poloxamer 407 gels. Pharm Res 14:309-13.

Ferreira, L., Vidal, M. and Gil, M. (2001). Design of a Drug-Delivery System Based On Polyacrylamide Hydrogels: Evaluation of Structural Properties J Chem Educ 6:100-3.

Fernandez, E., Lopez, D., Lopez, E. And Carmen, M. (2005). Viscoelastic and swelling properties of glucose oxidase loaded polyacrylamide hydrogels and the evaluation of their properties as glucose sensors. Polymer 46:2211-17.

Gil, M.H., Mariz, M., Puarte, M.G. (2002). Polymeric Biomaterials as Drug Delivery Systems. Boletim de Biotecnologia 72:13-9.

Gusbeth, C.A., Weaver, J.C. (2000). Non-linearity of molecular transport through human skin due to electric stimulus. J Control Release 68:373-86.

Huang, J., Song, K.C., Hu, O., Wang, J., Lin, Y., Fang, J. (2005). The effect of electrically assisted methods on transdermal delivery of nalbuphine benzoate and sebacoyl dinalbuphin ester from solutions and hydrogels. Int J Pharm 297:162-71.

Kantaria, S., Rees, G.D., Lawrence, M.J. (1999). Gelatin stabilized microemulsion-based organogels: rheology and application in iontophoretic transdermal drug delivery. J Control Release 60:355–65.

Korsmeyer, R.W., Gurny, R., Doelker, E., Buri, P., Peppas, N.A. (1983). Mechanism of solute release from porous hydrophilic polymers. Int J Pharm 15:25-35.

Lewus, R., Carta, G., Protien, G. (1999). Diffusion in charged polyacrylamide gels visualization and analysis. J Chromatogr A 865:155-68.

Lira, L.M., Torresi, C. (2005). Conducting polymer-hydrogel composites for electrochemical release devices: systhesis and characterization of semi-interpenetrating polyaniline-polyacrylamide network. Electrochem Commun 7:717-23.

Murdan, S. (2003). Electro-responsive drug delivery from hydrogels. J Control Release 92:1-17.

Peppas, N.A. and Wright, S.L. (1996) Solute Diffusion in Poly (vinyl alcohol)/Poly (acrylic acid) Interpenetrating Networks Macromolecules 29:8798-04.

Proikis, C., Mamouzelos, N., Tarantili, P. and Andrepoulos, A. (2006). Swollen and hydrolytic degradation of poly(D,L-lactic acid) in aqueous solution. Polym Degrad Stabil 91(3):614-19.

Sage, B.H., Riviere, J.E. (1992). Model systems in iontophoresis transport efficacy. Adv Drug Deliv Rev 9:265–87.

Sairam, M., Babu, R., Naidu, V., Aminabhavi, T. (2006). Encapsulation efficiency and controlled release characteristics of crosslinked polyacrylamide particles. Int J Pharm 320(1-2):131-36.

Tao,Y., Zhao, J. and Wu, C. (2005) Polyacrylamide hydrogels with trapped sulfonated polyaniline, Eur Polym J 41:1342-49.

Tanaka, T., Nishio, I., Sun, S. Ueno, S. (1982). Collapse of gels in an electric field. Science 218: 467 -69.

Valento, A., Burrows, H., Miguel, M. and Lobo, V. (2000). Diffusion coefficients of sodium dodecyl sulfate in water swollen crosslinked polyacrylamide membranes. Eur Polym J 38: 2187 -96.

Vankov, D. (2004). Diffusion of glucose and maltose in polyacrylamide gel. Enzyme Microb *Tech* 34:603-10.

Wang, K., Burban, H. and Cussler, E. (1993). Hydrogels as separation agents. Adv Polym Sci 110:67-79.

Yoshida, R., Sakai, K., Okano, T. and Sakurai, Y. (1993). Pulsatile drug delivery systems using hydrogels. Adv Drug Deliv Rev 11, 85-108.

ต้นฉบับ หน้าขาดหาย

Table 6.1 The molecular weight between crosslinks, the mesh size, and the crosslinking density of PAAM hydrogels at various crosslinking ratios with and without the electric field

Sample	Crosslinking ratio, X (mol_{MBA}/mol_{AAM})	Number-average molecular weight between crosslinks, M_c (g/mol)		Mesh size ξ (Å)		Crosslinking density ($mol/cm^3 \times 10^4$)	
		E = 0 V	E = 0.1 V	E = 0 V	E = 0.1 V	E = 0 V	E = 0.1 V
PAAM_0.002	0.002	8293 ± 339	33398 ± 3693	252 ± 7	348 ± 7	1.63 ± 0.07	0.41 ± 0.04
PAAM_0.005	0.005	4318 ± 21	34294 ± 397	158 ± 14	304 ± 5	3.13 ± 0.02	0.42 ± 0.01
PAAM_0.010	0.010	4050 ± 43	24031 ± 3823	128 ± 2	227 ± 16	3.33 ± 0.04	0.57 ± 0.09
PAAM_0.016	0.016	2700 ± 332	18196 ± 1058	85 ± 2	177 ± 5	5.04 ± 0.62	0.74 ± 0.04
PAAM_0.024	0.024	1555 ± 277	8752 ± 1903	57 ± 5	119 ± 4	8.82 ± 1.57	1.58 ± 0.34

Table 6.2 Diffusion coefficients in polyacrylamide hydrogels

Model drug	MW	Drug size (Å)	mol_{MBA}/mol_{AAM}	$D(cm^2s^{-1})$	pH	Temp.(°C)	E (V)	Membrane
Acetylsalycylic acid[a]	180	3.01	0.0115	1.2×10^{-7}	7	37	-	-
			0.2305	8.5×10^{-8}	7	37	-	-
Sodium dodecyl sulfate[b]	288	20	0.0320	0.5×10^{-6}	7	25	-	-
			0.0032	1.2×10^{-6}				
			0.0014	2.5×10^{-6}				
Hydrochlorides of ephedrine[c]	201	-	-	4.3×10^{-5}	-	15	-	-
Hydrochlorides of pethidine[c]	283	-	-	2.8×10^{-6}	-	15	-	-
Sodium chloride[c]	58	-	-	1.0×10^{-5}	-	15	-	-
Glucose[d]	180	32.7	0.0461	2.59×10^{-6}	7	60	-	-
			0.0922	3.23×10^{-6}	7	60	-	-
			0.1844	5.27×10^{-6}	7	60	-	-
			0.461	9.24×10^{-6}	7	60	-	-
Maltose[d]	342	20.95	0.0461	1.4×10^{-6}	7	60	-	-
			0.0922	2.11×10^{-6}	7	60	-	-
			0.1844	3.41×10^{-6}	7	60	-	-
			0.461	6.38×10^{-6}	7	60	-	-
Luteinizing hormone[e]	118	-	0.0115	1.64×10^{-7}	3.6	-	3 (0.6 mA)	Rat skin

a = Ferreira *et al.*,2001; b = Valento et al., 2000; c = Attwood *et al.*, 1981;d= Vankov et al., 2004;

e = Chen et al., 1996.

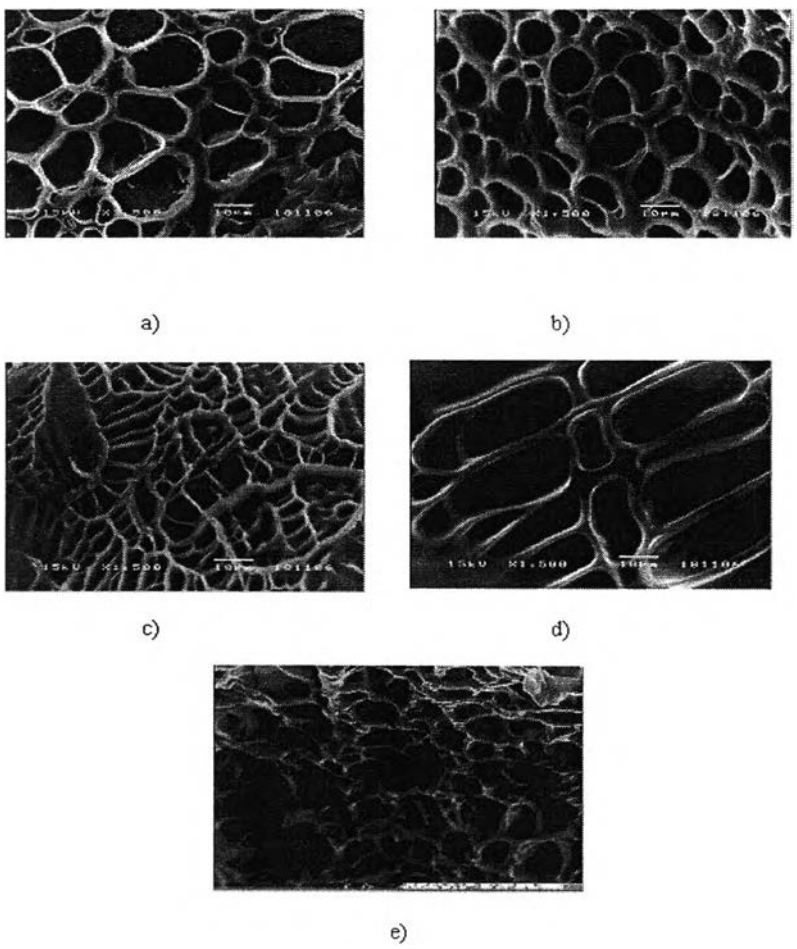

Figure 6.1 Morphology of PAAM hydrogel after swelling without electric field: a) PAAM_0.002; b) PAAM_0.005; and c) PAAM_0.016. Images d) and e) are the morphology of PAAM_0.016 after swelling under an electric field strength of 0.1 V (d) and 5.0 V (e), respectively at magnification of 1500.

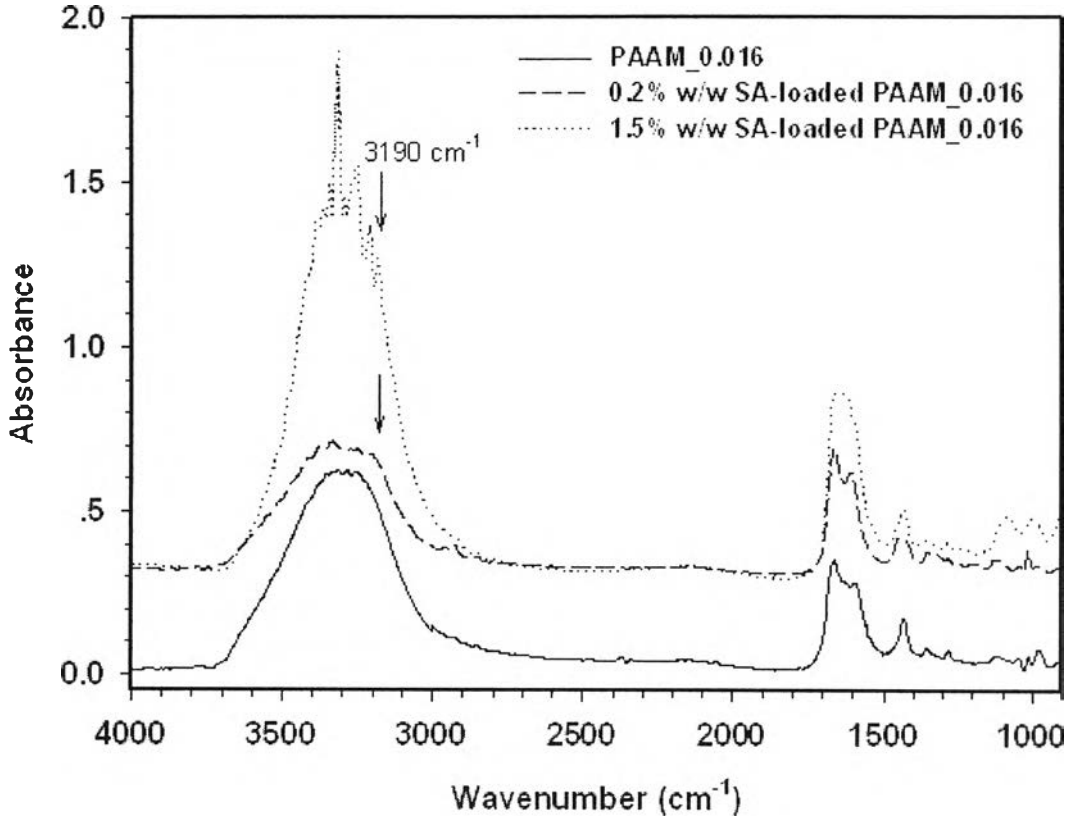

Figure 2 Absorption infrared spectra of a) PAAM hydrogel and b) 0.2% w/w SA-loaded PAAM hydrogel.

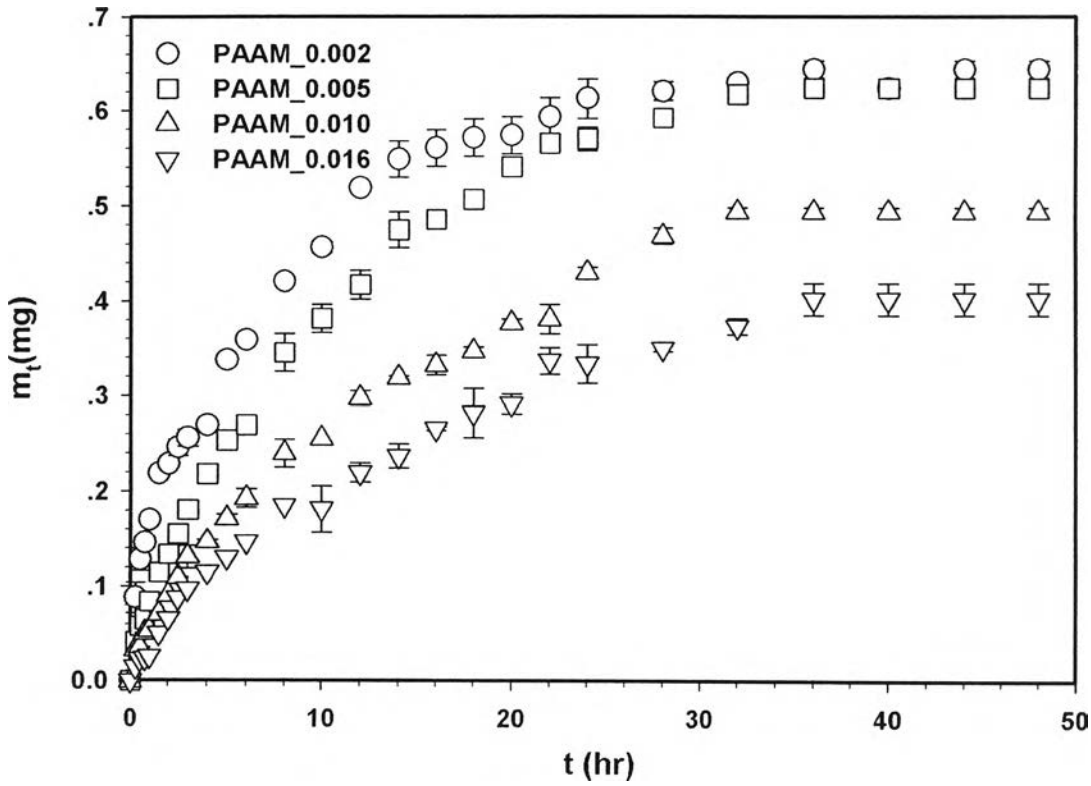

Figure 6.3 Amount of SA release from SA-loaded PAAM hydrogel at time t vs. t (hr) at various crosslink ratios, E = 0 V, pH 5.5, and at 37°C.

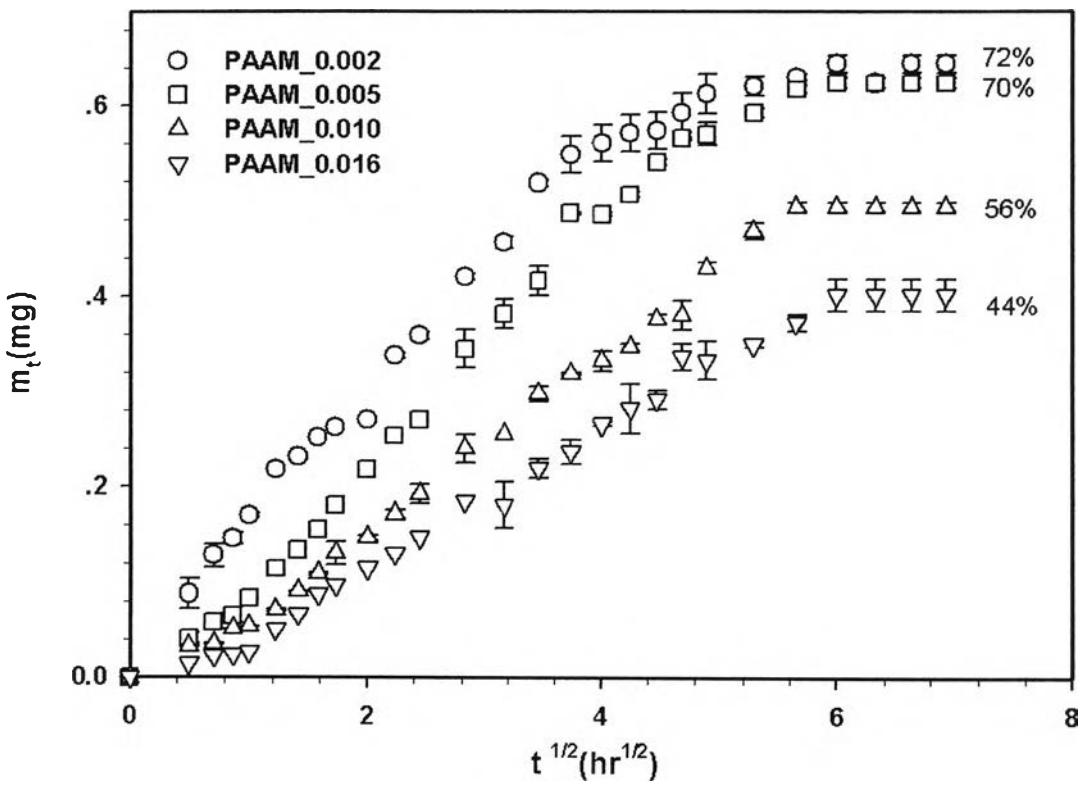

Figure 6.4 Amount of SA release from SA-loaded PAAM hydrogel at time t vs. $t^{1/2}$ ($hr^{1/2}$)at various crosslink ratios, E = 0 V, pH 5.5, and at 37°C.

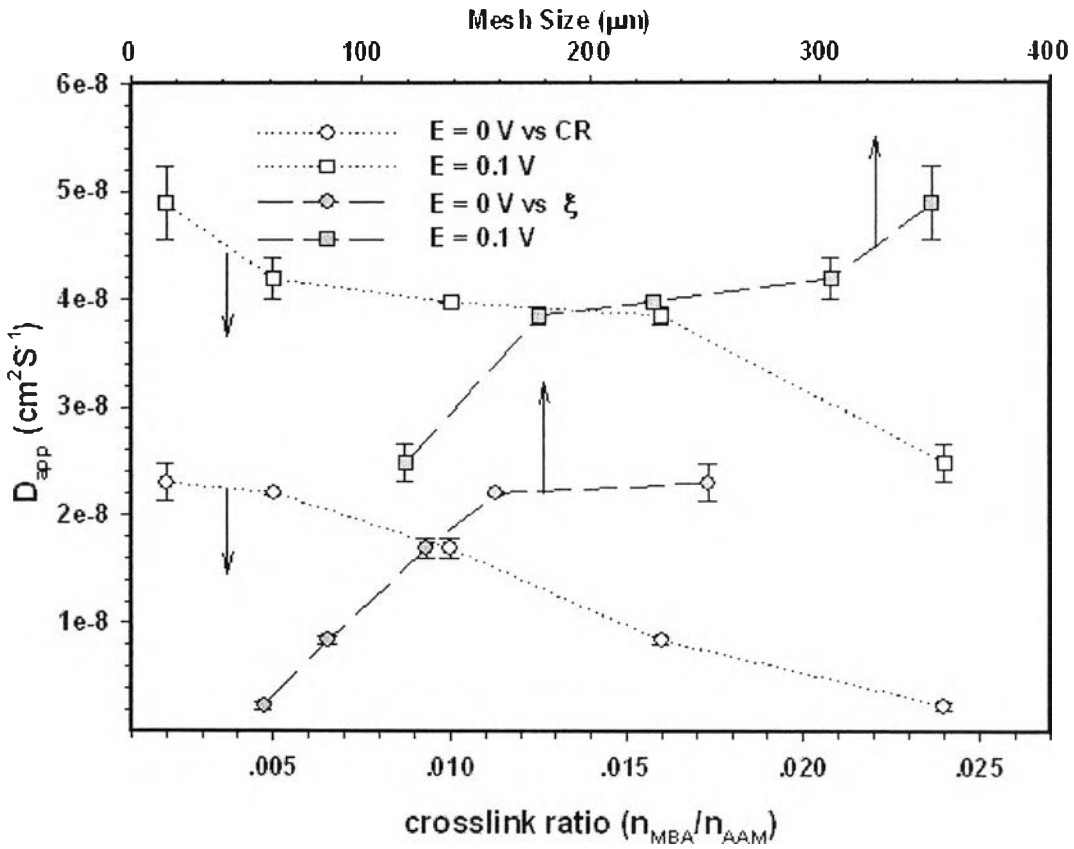

Figure 6.5 Apparent diffusion coefficient, D_{app} of SA from SA-loaded PAAM hydrogels vs. crosslink ratios and mesh size at an electric field strength of 0 and 0.1 V, pH 5.5, and at 37 °C.

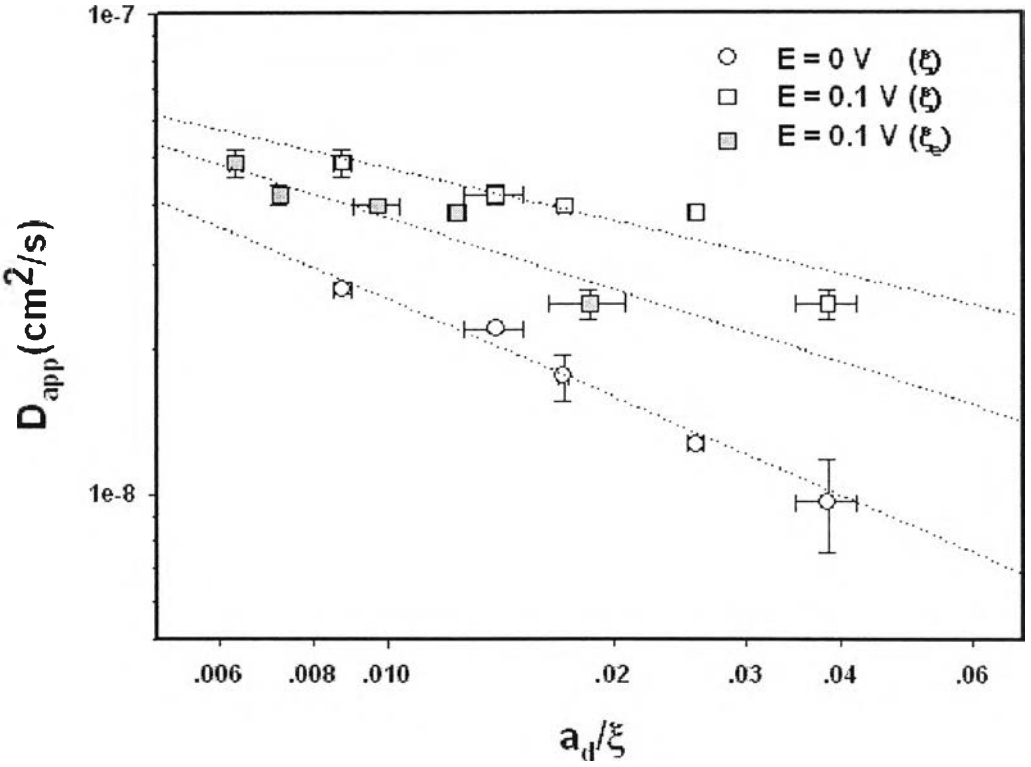

Figure 6.6 Apparent diffusion coefficient, D_{app} of SA from SA-loaded PAAM hydrogels vs. drug size/mesh size of hydrogel at an electric field strength of 0 and 0.1 V, pH 5.5, and at 37 °C.

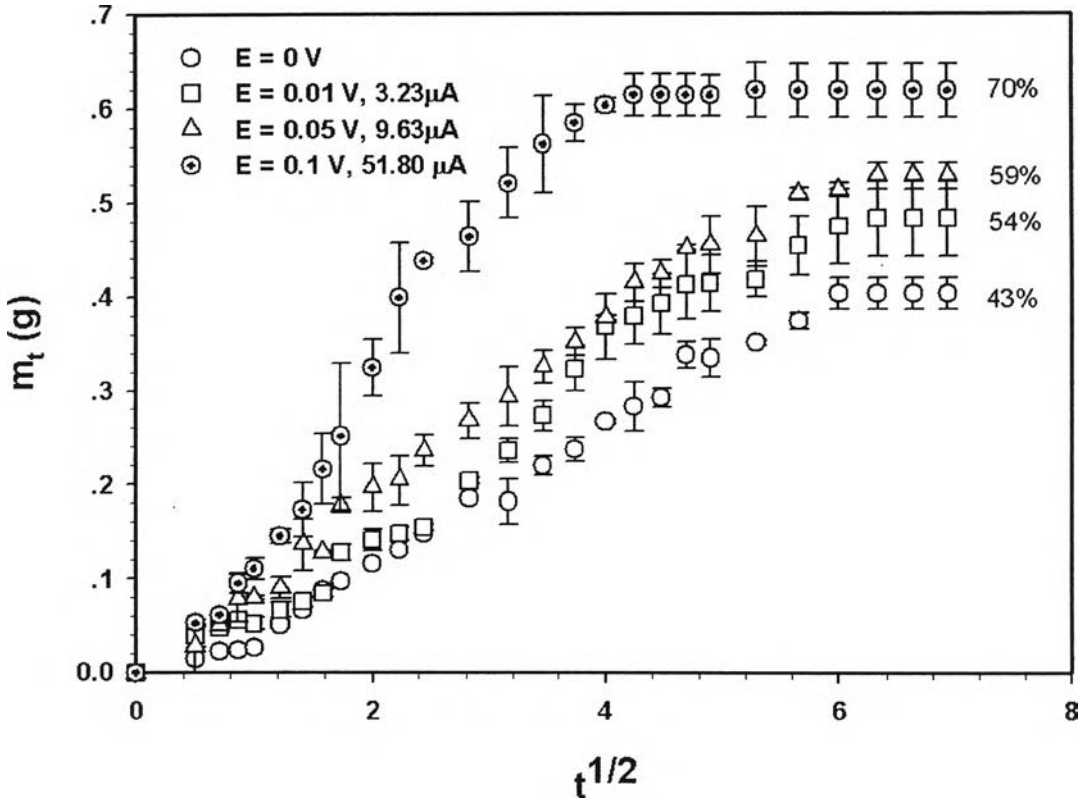

Figure 6.7 Amount of SA release from SA-loaded PAAM hydrogel (PAAM_0.016) at time t vs. $t^{1/2}$ at various electric field strength, pH of 5.5, and at 37°C.

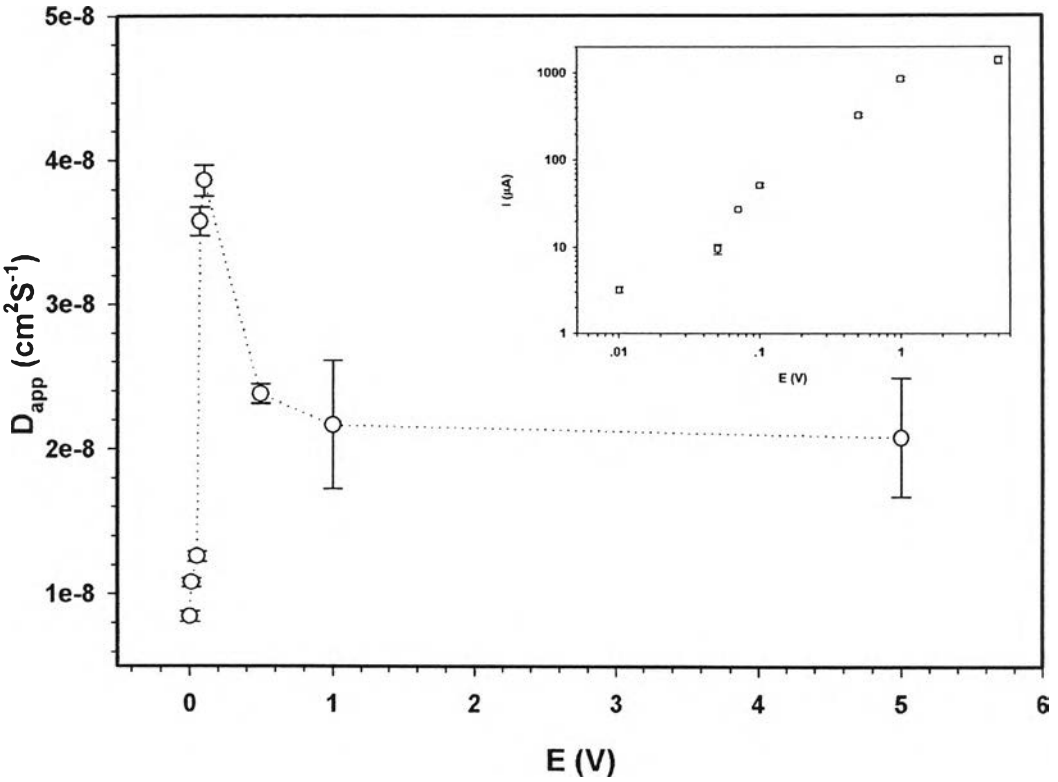

Figure 6.8 Apparent diffusion coefficient, D_{app} of SA from SA-loaded PAAM hydrogels (PAAM_0.016) vs. electric field strength at pH 5.5, and at 37 °C.